System Identification and Model based Performance Analysis of Hydrostatic Transmission System

Md Ehtesham Hasan[1]
S. K. Ghoshal[2]
Department of Mechanical Engineering
Indian School of Mines
Dhanbad, India
hasan.adab@gmail.com[1]
sanjoy.ghoshal@gmail.com[2]

K Dasgupta[3]
Department of Mining Machinery Engineering
Indian School of Mines
Dhanbad, India
dasgupta_k2001@yahoo.co.in[3]

***Abstract*—This article is aimed at system identification of a pedagogical hydrostatic transmission system (HST) through parameter estimation using constitutive relations and real measurements. A bondgraph model has been developed to analyze the performance of the system through system modeling and simulation. The characteristic curves for different components of the HST system were also obtained through simulation and validated experimentally.**

Keywords—Bondgraph, Hydrostatic transmission system, Performance analysis, System identification.

Basic Bondgraph symbols used in model

I ***Single port energy storage inertial element***

C ***Single port energy storage capacitive element***

R ***Single port dissipative element***

SF ***Single port element that indicates source of flow***

SE ***Single port element that indicates source of effort***

1 ***Common flow junction***

0 ***Common effort junction***

TF ***Two port element that converts hydraulic energy to mechanical energy and vice-versa***

I. INTRODUCTION

Hydrostatic Transmission (HST) systems provide infinite torque to speed ratio, an advantage over conventional power transmission using gears. While considering the use of an HST system, the dynamic characteristics of the transmission must be considered, whereas with the gear train such consideration is not often necessary. Dynamic performance of HST system has been studied through model simulation in [1-6]. The whole parameter set required for model simulation must be known a priori. When some of the parameters are unavailable, those must be estimated from test-data as a part of system identification. Nelles published a book dealing with many approaches for system identification based on neural network and fuzzy logic [7]. Yousefi has used Differential Evolution (DE) algorithm to obtain the best values for unknowns of a servo-hydraulic system [5].Czop et al. have used a linear transfer function to obtain the unknown parameters of a servo-hydraulic test rig [6]. Yan et al. [8] have used recursive lease square method to identify the unknown parameters of an electro hydraulic control system. Dasgupta et al. [9] had carried out model based dynamic performance of a closed-loop servo-valve controlled hydro-motor drive system using Bondgraph[10,14,15].

HST system is used for power transmission and efficiency of power transmission depends upon the performance of its components. Dynamics of flexible line in HST system play a dominant role in power transmission [11]. Other components like pump and motor affect the overall performance depending upon their operating parameters [12]. Power transfer also gets affected due to variation in bulk modulus of working fluid. The bulk modulus is affected by the air entrapment in the fluid [13].

The pedagogical HST system, considered for the present work, is an open loop system consists of hydraulic pumps, valve and motor. The system modeling [8,9] has been made using Bondgraph simulation technique [10,14,15]. The system equations derived from the model are solved numerically. While solving the equations, the parameters are estimated from the test data. The performance of the system with respect to the variation of the different parameters of the system is studied through simulation.

The paper is organized as follows. In the next section physical system has been described. Modeling of the system is described in Section 3. Identification of system parameters through experimentation is given in Section 4. Simulation results are discussed in Section 5 and finally conclusions are drawn in Section 6.

II. THE PHYSICAL SYSTEM

The system considered for the analysis is shown in Fig. 1, where a pressure compensated variable displacement pump (B) driven by a prime mover (A) supplies flow to the hydromotor (D) through proportional direction control valve (DCV). The DCV has 3 positions, direct and neutral positions are used to run the present experimental circuit while the cross position is used to run another circuit which is not in the scope of the present study.

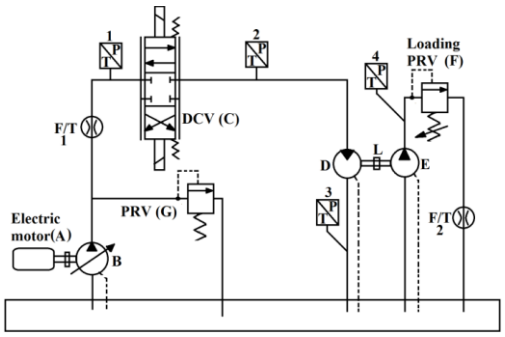

Fig. 1. The physical system

The hydromotor in turn drives the pump (E) that supplies flow to the tank through pressure relief valve (PRV). By adjusting the set pressure of the relief valve, the load on the hydromotor is varied. The pressure and the flow of the system are measured by the sensors (P/T and F/T) shown in Fig.1. Hydraulic motor speed is measured by using a proximity sensor. The pressure relief valve (G) protects the system against over pressure.

III. SYSTEM MODELING

The system is modeled by using Bondgraph [10,14,15] (Fig. 2), which has certain distinct advantages compared to other modeling techniques. When it comes to the modeling of systems that consists of sub-systems from different energy domains (like electrical, hydraulic and mechanical as applicable to the present system), the bond graph method is the convenient and efficient.

The assumptions considered for the model development of the physical system are as follows

- The fluid inertia is neglected.
- A constant velocity source to run the pressure compensated pump is considered.
- Hydraulic oil used is considered to be Newtonian fluid.
- The resistive and capacitive effects are lumped wherever appropriate.
- The effects of pressure on the properties of fluid are neglected.
- The leakages other than that from pumps and motor are neglected.

Referring to Fig. 2 the electric motor A is assumed to drive the pump (B) at constant speed (ω_s) represented by SF1. A transformer element (TF) in the Bondgraph representation of a hydraulic system transforms the hydraulic power to mechanical power and vice-versa. The TF elements connecting 1 and 0 junctions represent the volume displacement rate of the Pump (D_{mp}). The transformer modulus $D_{mp}(P_s)$ denotes the pump displacement rate which is a function of system pressure (P_s). The bulk stiffness of the fluid (K_m) is denoted by C element. The pump flow passes through proportional valve F (Fig. 2), which is represented as resistance R_8. The flow through the proportional valve depends on its port area A_{dcv}. The 1 junction indicating the mechanical part of the load corresponds to the speed of motor output shaft ω_m. The load inertia (J_1), speed dependant friction load (R_{fric}) are represented by I and R elements, respectively. They are connected with 1 junction that constitutes the load dynamics. The motor D is coupled with a pump E, and the mechanical energy is again converted to hydraulic pressure energy. The displacement of motor D and pump E is constant (D_m and D_p, respectively). The angular speed of the motor, and pressure of pump B, motor D, and pump E are measured as ω_m, P_s, P_{mi}, and P_{pp}, respectively. The flow from the pump E goes to tank H via relief valve F, the set point of which has been changed to load the system.

The system equations derived from the model are given below:

The flow supplied by the pump (B) is given by:

$$\omega_s D_{mp} = \frac{P_s}{R_{mplkg}} + C_d A_{dcv} \sqrt{\frac{2|P_s - P_{mi}|}{\rho}} + \dot{V}_{BL} \quad (1)$$

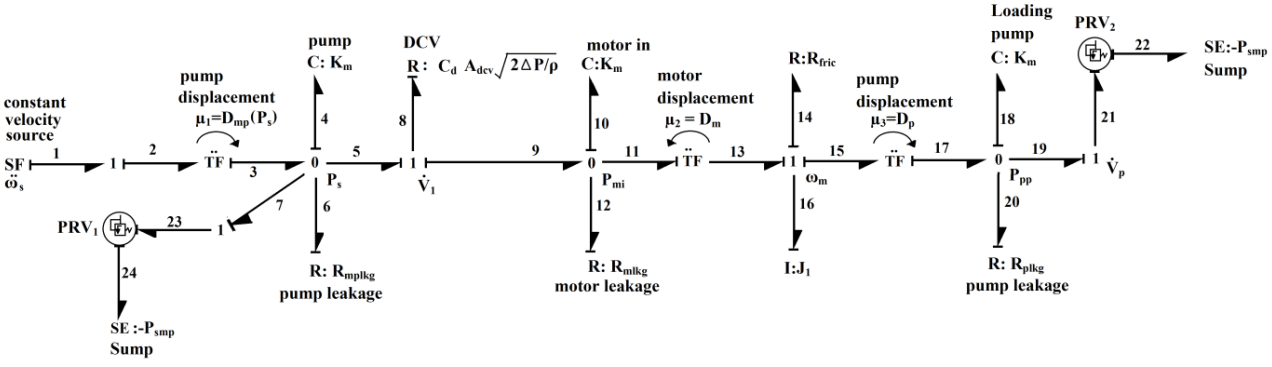

Fig. 2. Bond graph model of the system

Where the first term of the above equation represents ideal flow from the pump B, the second term is the leakage flow of the pump B, third term indicates the flow through the direction control valve (DCV), and the fourth term represents the compressibility flow loss of the fluid at the pump plenum.

The inlet flow to the hydraulic motor is expressed as:

$$C_d A_{dcv} \sqrt{\frac{2|P_s - P_{mi}|}{\rho}} = \omega_m D_m + \frac{P_{mi}}{R_{mlkg}} + \dot{V}_{DL}, \quad (2)$$

where the first term is the inlet flow to the motor that comes through the DCV. The second term represents the outlet flow of the motor. The third term and the fourth terms represent the leakage flow of the motor and the compressibility flow loss of the fluid at the motor plenum, respectively.

The 1 junction represents mechanical load part of the motor that comes from the torque balance, which is expressed by the following equation,

$$\dot{P}_1 = P_{mi} D_m - \omega_m R_{fric} - P_{pp} D_p \quad (3)$$

Where the first term of equation 3 i.e. ($\dot{P}_1$) is the torque due to inertia load J1, the second term i.e. $P_{mi} D_m$ indicates the torque equivalent to the pressure at motor (D) inlet, the third term i.e. $\omega_m R_{fric}$ is the torque loss due to viscous friction coefficient R_{fric}, the fourth term i.e. $P_{pp} D_p$ represents the torque applied on the motor (D) shaft due to pressure at loading pump (E) outlet.

The flow supplied by the pump (E) is expressed as

$$\omega_m D_p = \frac{P_{pp}}{R_{plkg}} + C_d A_{prv} \sqrt{\frac{2|P_{pp} - P_{atm}|}{\rho}} + \dot{V}_{EL} \quad (4)$$

Where the first term represents outlet flow from the pump (E), the second term indicates leakage flow of the pump (E), the third term is the inlet flow to the PRV and the fourth term indicates the compressibility flow loss of the fluid at the pump plenum.

The angular velocity of the motor (D) is given by:

$$\omega_m = \frac{P_1}{J} \quad (5)$$

The pressure at pump (B) outlet is expressed as

$$P_s = K_{pmp} V_{BL} \quad (6)$$

The pressure at the motor (D) inlet is given by:

$$P_{mi} = K_{pm} V_{DL} \quad (7)$$

The pressure at the pump (E) outlet is expressed as

$$P_{pp} = K_{pp} V_{EL} \quad (8)$$

IV. ESTIMATION OF THE PARAMETERS

Some parameters of the pump, motor and valves were obtained from test data and others are estimated theoretically. The bulk stiffness of the fluid at pump and motor plenum were considered identical and obtained theoretically. The displacements of the hydro motor (D) and the pump (E) were also obtained theoretically.

4.1 Flow-pressure characteristics of pump (B)

When the load pressure exceeds the set pressure, the swash plate angle of the pump decreases to near zero. A minimum angle of the swash-plate is required to maintain the leakage flow of the pump. However, the maximum and the minimum values of the swash-plate angle are restricted by the end stops and the pre-compression of the pump return spring.

The flow versus pressure of the pressure compensated pump (B) in the physical system was obtained through experimentation as shown in Fig. 3. It was construed from the characteristics in Fig. 3 that in region-1 flow rate decreased linearly with a constant slope due to the leakage of fluid from the pump plenum. Thereafter, when pressure approached the maximum limit (P_s=90×10^5 N/m^2), the drastic fall of flow rate was observed due to the pressure compensation. In the region-2 the nature of fall was observed parabolic, and in the region-3 it was almost linear. Based on this experimental observation, the flow-pressure characteristic of the pressure compensated pump was assumed to be a composite curve in three regions (Fig. 4) in the model. The equations representing the three regions were approximated as follows:

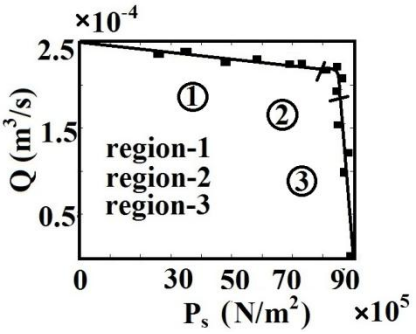

Fig. 3. Flow vs. pressure characteristics of pressure compensated pump (B) in the physical system

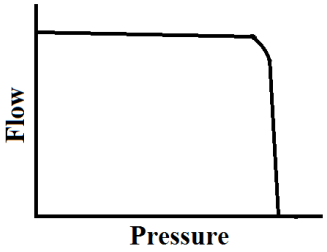

Fig.4: Flow vs. pressure characteristics of a typical pressure compensated pump

The equation for the region-1 of flow-pressure characteristic was obtained from linear fit of the test data and expressed as:

$$Q = -2.611 \times 10^{-14} P_s + 1.666 \times 10^{-6} \quad (9)$$

Where Q represents flow from the pump and P_s indicates the system pressure.

The equation governing region-2 was derived from quadratic fit of the test data and given as:

$$Q = -1.1 \times 10^{-18} {P_s}^2 + 1.7 \times 10^{-11} P_s - 6 \times 10^{-5} \quad (10)$$

The equation for the region-3 was obtained from linear fit and expressed as:

$$Q = 3.053 \times 10^{-12} P_s + 27.48141 \times 10^{-6} \quad (11)$$

4.2. Estimation of the port area of DCV

Two valves have been used in the set-up: one is the direction control valve (DCV) and other is the pressure relief valve (PRV). Although the pressure and flow across these two valves are obtained from the pressure and flow sensors, but the port areas of these valves cannot be measured directly. Therefore, the port areas are obtained using the following equation:

$$Q_{dcv} = C_d A_{dcv} \sqrt{\frac{2|P_s - P_{mi}|}{\rho}} \quad (12)$$

From Eq. (12)it is clear that the relation between $\sqrt{|\Delta P|}$ ($=\sqrt{\frac{2|P_s - P_{mi}|}{\rho}}$)is directly proportional to the flow through the valve ($=Q_{dcv}$).

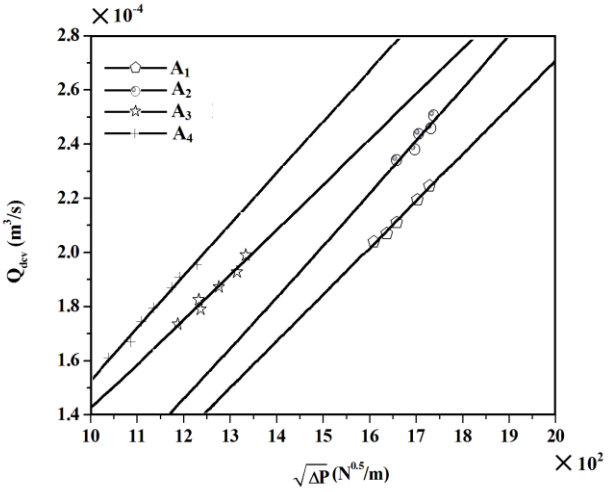

Fig. 5. Characteristics of $\sqrt{|\Delta P|}$ vs. Q_{dcv}

The characteristic of $\sqrt{|\Delta P|}$ vs. Q_{dcv} of DCV is shown in Fig. 5 The above results are obtained at different port opening areas (A_1 through A_4).

From the test data as shown in Fig. 5 the valve port opening areas are calculated, which are as given below:

$A_1 = 3.86 \times 10^{-6}$ m^2, $A_2 = 4.29 \times 10^{-6}$m^2, $A_3 = 4.43 \times 10^{-6}$ m^2, $A_4 = 4.77 \times 10^{-6}$ m^2

4.3 Estimation of port area of PRV

For a pressure relief valve the relation between flow and pressure drop across it is as follows:

$$Q_{prv} = C_d A_{prv} \sqrt{\frac{2|P_{pp} - P_{atm}|}{\rho}} \quad (13)$$

From Eq. (13) it is clear that $\sqrt{|\Delta P|}$ ($=\sqrt{\frac{2|P_{pp} - P_{atm}|}{\rho}}$) is directly proportional to the flow through the valve ($=Q_{prv}$).

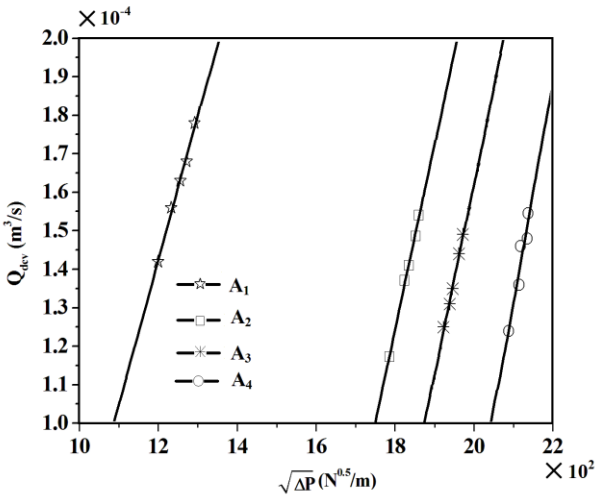

Fig.6.Characteristics of $\sqrt{|\Delta P|} vs. Q_{prv}$

The characteristic of $\sqrt{|\Delta P|}$ vs. Q_{prv} of PRV is shown in Fig. 6. The above results are obtained at different port opening areas (A_1 through A_4).

From the test data as shown in Fig. 6 the valve port opening areas are calculated, which are as given below:

$A_1 = 3.525 \times 10^{-6}$ m^2, $A_2 = 1.95 \times 10^{-6}$ m^2, $A_3 = 1.93 \times 10^{-6}$ m^2, $A_4 = 1.769 \times 10^{-6}$ m^2

V RESULTS AND DISCUSSIONS

The simulation was carried out to investigate the dynamic performance of the system. With the parametric values estimated through test data (as described in Sec. IV) and also obtained from product catalogue, the system equations given in Sec. III were solved numerically by using software Symbols-Shakti® [10,14,15]. All the parametric values assigned for the simulation are listed in Table 1.

5.1. Effect of variation of bulk modulus of the fluid.

Bulk modulus of fluid may change due to air entrapment. The effect of variation of bulk stiffness of the fluid (K_m) on the motor speed (ω_m) is shown in Fig. 7. With the increase in the value of K_m, the motor speed settled down at a faster rate.

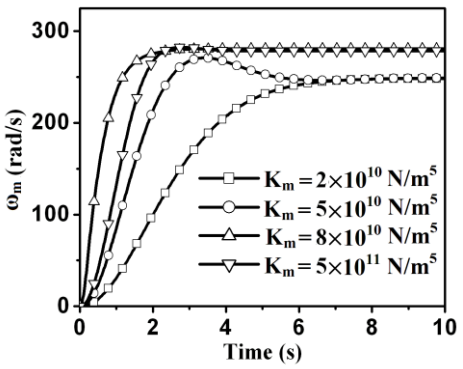

Fig. 7. Effect of varying bulk stiffness on the hydraulic motor speed

TABLE I. PARAMETRIC VALUES AND SET PRESSURE CONSIDERED FOR SIMULATION

Parameters	**Values**	**Parameters**	**Values**
Full open pressure for PRV_1	$13\times10^6 N/m^2$	Relief valve 2 set pressure	6×10^5 N/m^2
Full open flow for PRV_1	2×10^{-4} m^3/s	Pump (B) speed (ω_s)	150 rad/s
Density(ρ)	870 kg/m^3	Bulk stiffness of hydraulic oil (K_m)	1×10^{11}N/m^5
Relief valve 1 set pressure	8×10^6N/m^2	Pump (E) displacement	6.12×10^{-7} m^3/rad
Relief valve 2 full open pressure	8×10^5N/m^2	Motor (D) displacement	6.74×10^{-7} m^3/rad
Relief valve 1 full open flow	2×10^{-4} m^3/s	Main pump (B) displacement	1.33×10^{-6} m^3/rad
Damping ratio (ζ)	0.70	Frictional resistance	0.014 N
Motor leakage	6×10^{11} N.s/m^5	Pump leakage	6×10^{11} N.s/m^5
Moment of inertia of motor pump coupling	0.015 kg.m^2	Piston mass of relief valve	0.1 kg
Piston area of pressure relief valve	9×10^{-6}m^2	Atmospheric pressure (P_{atm})	1 bar

5.2. Effect of variation of port opening area of proportional DCV .

Figure-8 displays the speed response of hydro-motor (D) with varying port opening area of proportional DCV. It is observed from the figure that with increase in opening area of proportional valve the speed of hydraulic motor increases, although peak time almost remains same. This is because the rate of flow increases with port opening area of the valve.

5.3. Effect of variation of bulk stiffness on pump pressure.

Fig. 9 represents the pressure response across the pump B with increase in bulk stiffness. Although practically it is very difficult to change the bulk stiffness, since to change it the fluid must be changed or there must be significant change in temperature of fluid. In the above figure it is clear that with increase in the bulk stiffness the time taken to reach the maximum pressure reduces, as liquid acting as spring takes less time to transfer the applied force on it.

5.4. System identification

The speed response of hydromotor D obtained through simulation of the Bondgraph model using the parametersgiven in Table 1 and for a particular value of A_{dcv} (= 5×10^{-6}) is plotted in Fig. 10(a). The test data of the physical system were archived by using a portable data logger, HMG 3010, made by Hydac Electronics. The Data logger recorded speed of the motor D at every 2 millisecond, which is shown in Fig. 10(b).The plot of test data matches with the simulation result (Fig. 10(a)) with sufficient accuracy.

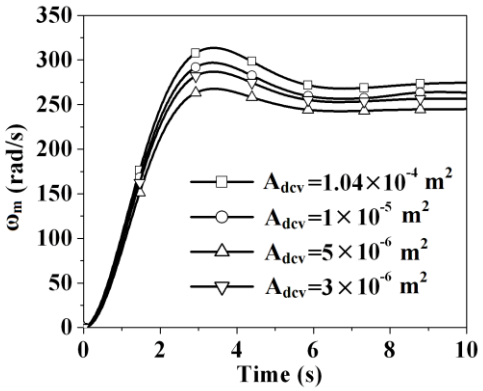

Fig. 8. Variation of speed with varying port opening area of proportional DCV

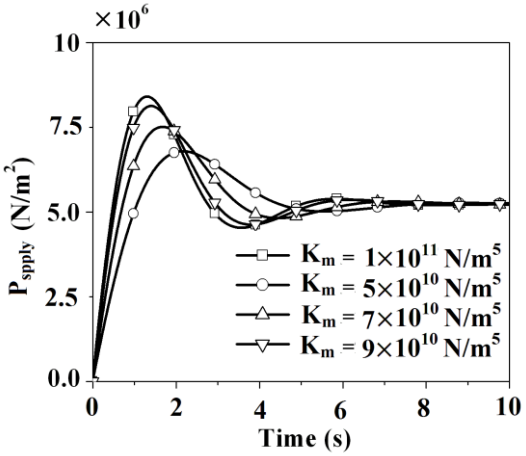

Fig. 9. Effect of change in bulk stiffness on pump pressure

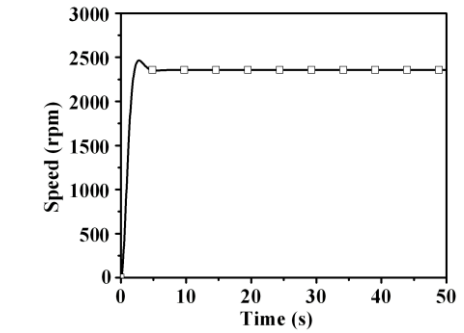

(a)

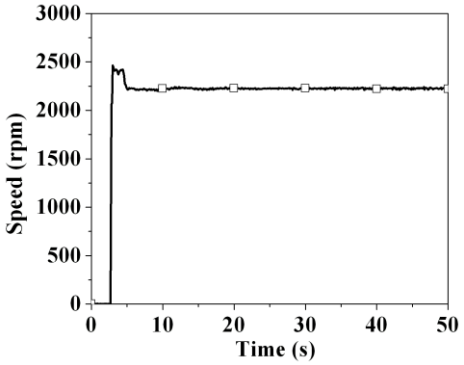

(b)

Fig. 10. Speed response of hydro-motor D; (a) Simulation, (b)Experimentation.

VI SUMMARY AND CONCLUSION

Estimation of some of the system parameters and performance analysis of the system have been done on an open loop pedagogical HST system. In this respect, the displacement of pressure compensated variable displacement pump (B) is modeled by using composite curves considering the flow variation both due to increased leakage at higher pressure and nonlinear pressure compensation effect. The port areas of the valves and the leakage resistance of the pump are estimated through test data. Using the parameter values obtained from experimentation and product catalogue, the simulation of the model has been carried out. The effects of critical parameters of the system on the speed and pressure responses on the system have been investigated. The work may be extended further for control analysis with an objective of best performance with respect to energy efficiency.

REFERENCES

[1] Dasgupta K, Watton J, Pan S. (2006), Open-loop dynamic performance of a servo-valve controlled motor transmission system with pump loading using steady-state characteristics, *Mechanism and Machine Theory*, Vol. 41 (2006), pp. 262-282.http://www.sciencedirect.com/science/article/pii/S0094114X05001102

[2] Dasgupta K., Analysis of hydrostatic transmission system using low speed high torque motor, *Mechanism and Machine Theory*Vol.35(2000),pp.1481-1499.http://www.sciencedirect.com/science/article/pii/S0094114X00000057

[3] Saber A. R., TutunjiT.,Identification and analysis of hydrostatic transmission system, *Int. J. Adv. Manufacturing Technology*, Vol.37,(2008),pp.221-229. http://link.springer.com/content/pdf/10.1007%2Fs00170-007-0966-3.pdf

[4] Sadegheih Ali, SazgarHadi, GoodarziKamyar, LucasCaro, Identificationand real-time position control of a servo-hydraulic rotary actuator by means of a neurobiologically motivated algorithim, *ISA Transactions* Vol. 51,(2012) : 208-219.http://www.sciencedirect.com/science/article/pii/S0019057811001157

[5] Yousefi H, Handroos H, Soleymani A (2008). Application of differential evolution of a servo hydraulic system with a flexible load.*Mechatronics*Vol.18(2008),pp.513-528. http://www.sciencedirect.com/science/article/pii/S095741580800041X

[6] Czop P, Wszolek G (2010). Advanced model structures applied to system identification of a servo hydraulic test rig. *Journal of achievements in materials and manufacturing engineering*. Vol. 41/1-2(2010),pp.96-103. http://www.researchgate.net/publication/49594025

[7] Oliver Nelles, Nonlinear System Identification: From Classical Approaches to Neural Networks and Fuzzy Models*Springer* 2001.http://www.springer.com/engineering/robotics/book/978-3-540-67369-9

[8] Yan J, Li B, Ling H-F, Chen H-S, Zhang, Nonlinear state space modeling and system identification for electro hydraulic control, *Mathematical problems in Engineering* (2013) id-970903.http://www.hindawi.com/journals/mpe/2013/973903/

[9] Dasgupta K, Murrenhoff H., Modeling and dynamics of a servo-valve controlled hydraulic motor by bondgraph. *Mechanism and Machine Theory,* Vol. 46(2011):1016-1035.http://www.sciencedirect.com/science/article/pii/S0094114X10000203X

[10] Mukherjee, A., Karmakar R. and Samantaray A.K. (2006). Bond Graph in Modeling, Simulation and Fault Identification. *I. K. International*: New Delhi, India.

[11] L. Yang, T. Moan., Dynamic analysis of wave energy converter by incorporating the effect of hydraulic transmission lines, *Ocean Engineering*Vol.38(2011)1849-1860. http://www.sciencedirect.com/science/article/pii/S0029801811002046

[12] Mandal S.K., Singh A. K., Verma Y., and Dasgupta K. (2012). Performance Investigation of Hydrostatic Transmission System as a Function of Pump Speed and Load Torque, *J. Inst. Eng. IndiaSer*. Vol. C,93(2), pp. 187-193.http://link.springer.com/content/pdf/10.1007%2Fs40032-012-0022-4.pdf

[13] AkkayaVolkanAli, Effect of bulk modulus on performance of hydrostatic transmission control system, *Sadhana*Vol.31, Part-5October2006,pp.543-556. http://link.springer.com/article/10.1007%2FBF02715913#page-1

[14] Mukherjee A. and Samantaray A. K. (2001). System modeling through bond graph objects on SYMBOLS 2000, *Proceedings ICBGM'01, SimulationSeries*,Vol.33,No.1, ISBN:1-56555-003-6,pp.164-170 http://citeseerx.ist.psu.edu/viewdoc/download?doi=10.1.1.84.5398&rep=rep1

[15] Karnopp D. Rosenburg R. C. (1978). System dynamics a unified approach.The University of Virginia.